Chronic and acute stress monitoring by electrophysiological signals from adrenal gland

Sung Hyuk Sunwoo[a,b], Ju Seung Lee[c], SungJun Bae[a,b], Yiel Jae Shin[c], Chang Seong Kim[d], Soo Yeon Joo[d,e], Hong Sang Choi[d], Minah Suh[a,b], Soo Wan Kim[d], Young Jin Choi[e,1], and Tae-il Kim[b,c,1]

[a]Center for Neuroscience Imaging Research, Institute of Basic Science, 16419 Suwon, Korea; [b]Department of Biomedical Engineering, Sungkyunkwan University (SKKU), 16419 Suwon, Korea; [c]School of Chemical Engineering, Sungkyunkwan University (SKKU), 16419 Suwon, Korea; [d]Department of Internal Medicine, Chonnam National University Medical School, Gwangju 61469, Korea; and [e]Department of Nanotechnology and Advanced Materials Engineering, Sejong University, 05006 Seoul, Korea

We present electrophysiological (EP) signals correlated with cellular cell activities in the adrenal cortex and medulla using an adrenal gland implantable flexible EP probe. With such a probe, we could observe the EP signals from the adrenal cortex and medulla in response to various stress stimuli, such as enhanced hormone activity with adrenocorticotropic hormone, a biomarker for chronic stress response, and an actual stress environment, like a forced swimming test. This technique could be useful to continuously monitor the elevation of cortisol level, a useful indicator of chronic stress that potentially causes various diseases.

biosensor | cortisol | electrophysiology | bioimplant | stress

Living organisms mainly use nervous and endocrine (hormonal) systems to control the body and maintain homeostasis. Both of these systems are normally independent. They perform unique functions to affect specific body parts. Endocrinal signals based on the flow of special chemicals called hormones affect the body chronically and massively. On the other hand, a neural signal based on electrophysiological (EP) potential changes of neuron cell membrane affects the body acutely and locally. For example, when the brain recognizes an external stress factor, both the neural and hormonal systems simultaneously respond through different pathways (Fig. 1A) (1). The neural signal is transferred to the adrenal medulla, which produces neurotransmitters called adrenaline to temporarily enhance neural and muscular activities under acute response. Meanwhile, the hypothalamus releases corticotropin-releasing hormone to the pituitary gland that generates adrenocorticotropic hormone (ACTH), which flows into the adrenal cortex, especially the adrenal zona fasciculata (AZF) cell in the adrenal gland (2, 3). The adrenal cortex then produces cortisol, a stress hormone that rebalances the body functions and performances of the neural and muscular system, as mentioned above (4). These serial flows of cortisol synthesis from the hypothalamus to the pituitary gland and adrenal cortex are also called the hypothalamus–pituitary gland–adrenal cortex (HPA) axis. The HPA plays an important role in long-term stress response. The HPA axis causes various reactions, such as increased blood pressure and heart rate, and enhanced immune system, in an organism in response to stress. However, repeated and chronic stress can cause malfunctions in the HPA axis (5, 6). Chronic stress involves the accumulation of excessive and unnecessary cortisol that eventually causes several diseases, such as amnesia (7), depression (5, 6), fatigue (8), anxiety (9, 10), and heart disease (11). Moreover, failure to control cortisol secretion also indirectly induces symptoms of autoimmune diseases (12), skin inflammation (13), type 2 diabetes (14), obesity (15, 16), sexual dysfunction (17, 18), and chronic pain (19). It is necessary to continuously monitor the cortisol concentration to prevent such diseases that are caused by chronic stress.

Although currently applied electrochemical analysis and enzyme-based analysis (20–23) using body fluids (blood, saline, and urine) have been widely applied, they still have important limitations for continuous cortisol detection. Because they require invasive access to patient's blood using disposable diagnostic kits, repeated measurement causes stress and pain. Moreover, electrochemical methods are not capable of real-time measurement, since there is a time gap between the abnormal cortisol secretion and the measurement for precise diagnosis (24–26). Recently, it was revealed that the EP signal induced by ion flux through the cellular membrane was responsible for the hormone-releasing process in the corresponding endocrine organs (Fig. 1A and SI Appendix, Fig. S1) (27–30). We assumed that accurate recording of an electric signal representing the physiological activities of endocrine cells could be applied to characterize cortisol change. Because conventional rigid in vivo EP sensors and devices made of silicon or metals may cause mechanical mismatch when implanted into soft tissue (31–34), they cannot be simply applied to the endocrine system, due to the anatomical characteristics of the adrenal gland and the other endocrine organs that are located in the deep internal area of the body (35, 36). Such mechanical mismatch can cause serious damage to the tissue, as well as cause mechanical failure of the device itself (SI Appendix, Fig. S2).

Thus, herein we demonstrate a longitudinally implantable flexible probe that can be used to quantify the relationship between the cortisol releasing level and EP signals from the adrenal gland based on flexible EP sensors. We found significant EP signal change when cortisol was released in ACTH injection, or an actual stress environment, like a forced swimming test. Our experiments were done using specially designed flexible EP probes that could penetrate the adrenal gland. Four electrodes on the probe are able to continuously measure EP signals in both the adrenal cortex and medulla area, and they allow us to successfully determine the activities of hormonal cells and relative

Significance

In this paper, we designed a flexible electrophysiological probe that could be implanted in the adrenal gland of a living animal. It allowed us to measure the electrophysiological signals of the adrenal gland in response to stress hormone release induced by acute stress. This report collects electrophysiological signals of the adrenal gland in vivo with chronic implantation.

Fig. 1. Schematic of the implanted device on the adrenal gland of a rat. (*A*) The scheme describing the stress response mechanism. When the brain recognizes the stress situation, neural and hormonal signals are transmitted from the brain to the lower organs, which represent acute and chronic responses, respectively. The adrenal medulla and adrenal cortex receive neural and hormonal signal, respectively, and perform the acute and chronic responses to stress. (*B*) The device is implanted in the dorsal part of the abdominal cavity (*Left*). The probe and the connector are linked with a conventional FFC (*Right*). (*C*) Detailed schematics of the sectional view of the adrenal gland and implanted probe. (*D*) The image of the probe taken by the optical microscope, and the relative sectional view of the adrenal gland. The four electrodes each have 700 μm of intervals (window size; 10 μm × 10 μm), so that they are able to cover both the cortex and medulla. (Scale bar in *Inset*: 50 μm.) (*E*) Schematic describing the structural information of the probe. (*F*) Photo image of the probe (yellow guideline) penetrating the adrenal gland (black dotted circle). The arrowhead tip fully penetrates the adrenal gland. (*G*) Photo image of the pins of the connector after implantation. Pin-based connection minimizes the possibilities of inflammation, and enables long-term recording.

change of cortisol hormone level under a stress environment in in vivo animal model.

Result

Preparation of EP Probe for Adrenal Gland. We fabricated flexible probes that could be implanted into the adrenal gland of a living animal (Fig. 1*B*). The probe contains a sensor with four-channel electrodes, flexible flat cable (FFC; Elform Inc.), and printed board circuit connector with four pins for the percutaneous link. Thin (60 μm) and flexible FFC (∼70 mm length) links were made between the probe and the connector. The whole probe was implanted in the abdominal cavity of an animal. Only the metal pins of the connector were exposed on the skin to transmit data to the external data acquisition device. The sensor part contains an arrowhead tip, shaft, and in and out (I/O) pads. The arrowhead tip helps the probe easily penetrate through the adrenal tissue. Once it has fully penetrated, the hook of the arrowhead anchors onto the adrenal capsule, so that the probe can be stuck in the implanted site (Fig. 1*C*). All materials used in fabrication had proven to be biocompatible (37–44). Four metal electrodes with 50 nm of gold (Au) and 20 nm of chromium (Cr) were patterned on the 5-μm-thick polyimide (PI) substrate using a conventional photolithography technique. Then, a 2-μm epoxy (SU-8 2; MicroChem) encapsulation layer covered the whole electrode layer, except for the recording Au electrode window (10 μm × 10 μm), and the I/O pads (250 μm × 5 mm). These four channels of gold electrodes were positioned along the shaft (150 μm width) with 700-μm intervals. The first and fourth electrodes were

designed to have contact with the adrenocortical tissue, while the other two electrodes were designed to have contact with the adrenomedullary tissue in ideal implantations (Fig. 1 *D* and *E*) (45, 46). *SI Appendix*, Figs. S3 and S4 describe the more detailed information of the probe fabrication and structure.

Implantation of the EP Probe into the Adrenal Gland. For the in vivo animal test, the probe was implanted into the adrenal gland of an anesthetized 8-wk-old male rat by dorsal incision (Fig. 1 *F* and *G*). After the probe had fully penetrated the adrenal gland as shown in the schematic illustration of Fig. 1*C* and photo image of Fig. 1*F*, it was fixed on the adrenal gland capsule by anchoring the arrowhead tip onto the opposite side of the fibrous capsule layer of the adrenal gland (Fig. 1*F*) (47, 48). After the probe was locked, we mechanically broke the shaft of the shuttle, so that we could remove the thick shuttle layer simply by retreating backward (*SI Appendix*, Fig. S5). Consequently, only the thin and flexible sensor layer (∼7 μm) remained inside of the adrenal tissue. The flexibility of the PI material and ultrathin nature of the sensor guaranteed minimized invasion with smaller biological damage. The four pins of the connector were exposed from the sutured skin after the surgery, while the rest of the system was submerged (Fig. 1*G*).
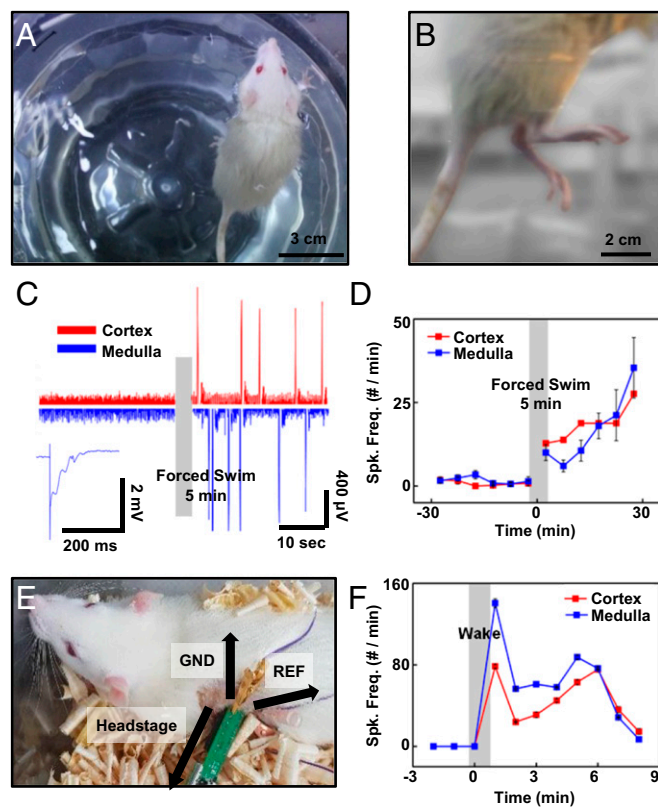
EP Signal Change in Adrenal Gland by ACTH Stimulation. Before we collected EP signals from the adrenal gland in vivo, we measured the EP signals from an enucleated adrenal gland in vitro (*SI Appendix*, Fig. S6). We implanted the probe into the enucleated adrenal gland with the saline in a Petri dish. We then

measured the signal of the adrenal gland as a reference, using a commercialized data-collecting instrument for about 30 min. Next, we added 60 ng of ACTH into the saline medium. The amplitude and frequency of the electric spikes recorded from the adrenal gland were significantly increased after ACTH addition.

First, we implanted the adrenal probe into the 8-wk-old SD (Sprague–Dawley) rats, and rehabilitated them for a week. After the week of recovery, we anesthetized the rats with urethane, then left them alone for an hour, to avoid the residual stress effect induced by the handling and preparation. Minimizing the signal noise from the animal's physical movement can help precise measurement of the EP signal. Then we recorded the reference EP signal (base-level signal without ACTH) for (30 to 60) min. We i.v.-injected 120 ng of ACTH through a catheter, and observed the EP spike activities in both adrenal cortex (red) and medulla (blue) after an ACTH injection (Fig. 2 *A* and *B* and *SI Appendix*, Fig. S7). As described in Fig. 1*A* and *SI Appendix*, Fig. S1, an increase of ACTH concentration in blood can actively excite adrenocortical cells to increase cortisol secretion, as well as induce chronic stress-like responses, such as increased glucose concentration. With this mechanism, we observed that the adrenal gland showed increased spike frequencies after ACTH injection, especially in the cortex. Fig. 2*B*, *Inset* shows a single spike from the adrenal cortex without high-pass filtering. With quantitative analysis, we counted the number of spikes per minute and found a significant increase of adrenal cortex activity after a 180-ng ACTH injection in 11 rats (Fig. 2*C*). To guarantee the EP signal was collected from the adrenal gland, we implanted two identical probes in different organs—adrenal gland and spleen—and compared signals after ACTH injection (*SI Appendix*, Fig. S8). The spleen was chosen as a control since it is located in the abdominal cavity near the adrenal gland, and also plays a role in an acute stress reaction, but does not respond to ACTH. Even after 180 ng of ACTH was injected, the recorded

EP signal from the spleen was still absent. Thus, we concluded the ACTH-responsible signal is the adrenal cortex-specific.

Based on data of EP signals induced by ACTH (Fig. 2 *B* and *C*), the quantitative relationship between the number of EP spikes and cortisol exocytosis was obtained (Fig. 2*D*). We collected blood samples five times per rat at different time points: before (−30 and 0 min) and after (30, 60, and 90 min) a 180-ng ACTH injection. Cortisol level measured with an enzyme-based cortisol sensor was gradually increased after ACTH injection (20). It was saturated at 125 nM at ~60 min after ACTH injection, as presented earlier (4). When the cortisol level increases, the blood glucose level also elevates. We measured the blood glucose level with the commercialized glucose detector (Accuchek; Roche) during adrenal spike recording. The blood glucose level was also elevated as the spike frequencies increased to high after ACTH injection (Fig. 2*E*). To find a more quantitative relationship between ACTH and EP signals, we injected saline solution containing various concentrations of ACTH ranging from 0 to 240 ng and measured EP signals of the adrenal cortex (Fig. 2*F*). In the case of normal saline injection (0 ng of ACTH) as a control experiment, the number of spikes of EP signal was slightly suppressed compared with that in the ACTH injection group. This is because saline injection caused dilution of the ACTH concentration and eventually decreased the ACTH level in the blood. On the other hand, various doses of ACTH (60, 120, and 240 ng) caused the increase of spike frequencies as the ACTH concentration increased. Interestingly, the frequency of cellular activity (EP signals) of the adrenal cortex was closely related to the ACTH level in the blood. Fig. 2*G* shows adrenocortical signal changes in the presence of cortisol antagonist, cycloheximide (49) and ketoconazole (50–52). We gave 1 cc of saline (control), 50 μg of cycloheximide in 1 cc of saline, and 20 mg of ketoconazole in 1 cc of dimethyl sulfoxide (DMSO) to each rat group by i.p. injection. Although we injected a sufficient amount of ACTH (180 ng), EP spikes were not notably detected

Fig. 2. Signal collected from adrenal gland after ACTH injection. (*A*) Conceptual schematic of the signal recording. When ACTH binds to AZF cell receptor, ion exchanges occur within the cell membrane. The probe records the potential changes of the surrounding cells, which represent cellular activities responding to the ACTH concentration. The collected signal passes through the commercialized head stages, including an amplifier, and is then recorded on the external device. (*B*) EP signals from the adrenal cortex (red) and medulla (blue) before and after ACTH injection. The number and amplitude of the spikes increased after a 180-ng ACTH injection. *Inset* shows a magnified image of the single spike. (*C*) The time course changes of the average spike frequencies per minute in the adrenal cortex before and after ACTH injection for 11 rats. Spk. Freq., number of EP spikes per minute. (*D*) The stress hormone, cortisol, concentration measured by an electrochemical sensor with blood sample during ACTH injection. The calculated blood cortisol level is shown. (*E*) Glucose level, which is mainly related to the concentration of cortisol change, is measured during ACTH injection. (*F*) Comparison of average number of spikes per minute after injection of various doses of ACTH. (*G*) Comparison of spike frequencies after injecting ACTH with inhibitors. We injected saline only (black), DMSO only (red), cycloheximide (CHX) in saline (green), and ketoconazole (KZ) in DMSO (blue) into the rat, and compared spike frequencies after the ACTH injection.

for the cycloheximide and ketoconazole group, while spike frequencies of the control group with the injection of only saline or DMSO were significantly elevated. Thus, there is an important relationship between the adrenocortical EP signals we collected from the flexible implantable probe and quantitative cortisol secretion. All EP signal data were achieved by multiple trials of experiment (*SI Appendix*, Fig. S9).

EP Signal in Adrenal Gland by Acute Stress. We also measured EP signal change in the whole adrenal gland induced by actual stress. The probe was implanted into the adrenal gland of male rats, and they were rehabilitated for 2 wk. After 2 wk of recovery, we collected the initial EP signal of the adrenal gland as reference data, as described in *EP Signal Change in Adrenal Gland by ACTH Stimulation*. Then the animal was gently placed into a bath with water level 30 cm from the bottom for a forced swim test (Fig. 3 *A* and *B* and *SI Appendix*, Fig. S10). After 5 min of swimming, we anesthetized the rat for EP recording. Interestingly, the EP signal was present in both the adrenal cortex and medulla (Fig. 3 *C* and *D*), unlike the ACTH injection cases (53–55). The blood catecholamine concentration declined slowly until the animal was fully recovered during the poststimulation

period (54, 56, 57). Also, since the animal was wet and hypothermic, active hormonal and neuronal signals were still recorded from the adrenal gland. We also anesthetized rats with the short-lasting anesthetic ketamine, and quickly connected the connector for communication. After 2 min of recording, the rats started to wake up, and freely moved around the cage (Fig. 3 *E* and *F* and *SI Appendix*, Fig. S11). Thus, we conclude that the probe is also applicable for identifying both neural and hormonal pathway responses.

Longitudinal Implantation for Chronic Monitoring. For longitudinal monitoring with chronic implantation, minimized inflammation and less invasiveness of the tissue and chronic stability of the probe must be ensured. It is obvious that ultrathin microscale geometry for minimal invasion and longitudinal interlocking with hook-shaped structures through the organ are beneficial for long-term recording. We prepared two animal groups with the adrenal probe. For one group, there remained an ~7-µm-thick substrate, after removing a thick and rigid shuttle. For the other group, we left the 250-µm-thick shuttle among the adrenal tissue. After 2 wk of implantation, the animals were fully recovered in appearance (Fig. 4*A*), and their survival rate for 2 wk was 98.2% (*n* = 165). We also examined H&E stained adrenal gland slices (40 µm in thickness). Compared with the bare adrenal slice without any implantation (Fig. 4*B*, *Top*) as a reference, adrenal slices with a shuttle showed massive tissue dissipation induced by mechanical damage, and scar tissue around the shuttle (Fig. 4*B*, *Middle*). However, on the adrenal slices without shuttle, the adrenal tissue had fully recovered without any significant damage (Fig. 4*B*, *Bottom*). The quantitative analysis compared the cross-sectional area of the vacant tissue and scar tissue between the adrenal group with and without shuttle among 20 slices of adrenal tissue per group (Fig. 4*C*). Adrenal slices at 1 wk (black solid) and 2 wk (red solid) after implantation (with a rigid shuttle) showed no noticeably different tissue damage. However, adrenal slices at 2 wk after implantation (blue solid; without a rigid shuttle) showed negligible damage. Scarring by the damage can also support this result (black dash, 1 wk implantation; red dash, 2 wk after implantation with rigid shuttle; and blue dash, 2 wk after implantation without the rigid shuttle; more detailed statistical data for surgery survive are in the legend of *SI Appendix*, Fig. S9). This result shows that removing the shuttle allows minimized invasion and damage of the adrenal gland, and is thus suitable for long-term implantation.

We also compared the EP signal and impedance in the first week and the ninth week after surgery, as the EP signal acquisition quality was reliable for long-term implantation (Fig. 4*D*). We observed signal increases after a 180-ng ACTH injection. The flexible nature of the probe can sustainably work due to minimized side effects, even with animal movement during implantation. Flexible substrate also helps maintain the low impedance of the electrode (Fig. 4*E*). The impedance of the conventional needle-shaped probe increased rapidly at around (4, 5) wk after implantation, due to the breakdown of the probe and tissue inflammation. However, the arrowhead anchoring probe maintained its impedance over 13 wk after implantation.

To find out the overall biocompatibility of the probe, we implanted the probe on the left, right, and both adrenals, and compared the weight changes with the control animal (Fig. 4*F*). There were no significant differences in weight change between the four groups. Since the adrenal gland plays an important role in animal metabolism, this result shows that the probe did not affect the function of the adrenal gland. We also checked whether the implanted probe might cause physical or mental stress to the animal. We monitored animal behavior in an open-field cage and traced their locomotive motion (Fig. 4*G*). We set an open-field cage of (60 cm × 60 cm) in the darkroom, and let the control rat and implanted rat freely move in the cage. In comparing the moved distance and average locomotion speed of the two groups of rats, there was no significant difference

Fig. 3. Adrenal probe application to the actual stress model. (*A* and *B*) Images of a rat with forced swimming test to apply acute stress. (*C*) EP signals collected from the adrenal cortex and adrenal medulla before and after the forced swim. The adrenal cortex signal after the forced swim (red) is enhanced compared with the one before the 5 min forced swim. Compared with ACTH injection, EP signal in the adrenal medulla (blue) is dramatically activated by the acute stress. (*D*) The forced-swim mediated signal elevation. The number of spikes per minute from the adrenal cortex (red) before and after swimming far increased after swimming, just as the number of spikes per minute of the adrenal medulla (blue) changed after swimming. (*E*) The image of a freely moving rat whose connector was linked to a commercialized head stage to collect the adrenal gland signal. (*F*) The signal was collected from the adrenal cortex and medulla before and after waking up from the anesthesia. Spike frequencies from the cortex and medulla were both elevated right after waking.

Fig. 4. Biocompatibility test for the adrenal probe. (*A*) The rat was fully recovered only 2 wk after surgery. *Inset* shows the magnified image of the pins of the connector after brief shaving. (*B*) The microscopic image of the H&E stained adrenal gland slice and camera image of the slice with (*Middle*) and without (*Bottom*) shuttle. The image shows the control adrenal slice that had not implanted any probe (*Top*). We observed a large dissipation of the tissue and scar around the shuttle (blue dashed box and white arrow) remained in the adrenal (*Middle*). In contrast, there is no noticeable damage around the remaining thin (a few micrometers) probe (yellow arrow), and the penetrated tissue is fully recovered (*Bottom*). In the camera image, the SU-8–based shuttle is clearly observed in the tissue, while there are no noticeable differences in the bare adrenal gland and adrenal gland without a shuttle. (*C*) Cross-sectional area of the damaged tissue area was measured with computer software. Tissue with shuttle showed a large dissipated area and scar tissue, while there was no clear damage in the tissue without shuttle. (*D*) The spikes of the adrenal cortex collected for long-term implantation. There were no significant differences before and after ACTH injection between 1 wk after implantation (black) and 9 wk after implantation (red). (*E*) Comparison of the impedance of the flexible arrowhead anchor probe with a conventional rigid probe. The impedance of the rigid probe increased rapidly around 4 wk after implantation (black) by the device breakage, while the impedance of the arrowhead probe was maintained for 13 wk after implantation (red). (*F*) The time course animal body weight changes. The body weights of the control group (black), left adrenal implant (red), right adrenal implant (green), and both adrenal implants (blue) show no noticeable differences over time. (*G*) Movement tracking of the rat with the implanted probe in the open-field cage (*Left*). The recorded trail of the animal movement within 5 min in the open-field cage of the control group (*Middle*) and the implanted group (*Right*). (*H*) Comparing the moved distance (bar, left axis) and the average velocity (red line, right axis) of the control group and implanted group of rats in the open-field cage.

between the two groups; we then concluded that the probe did not cause serious damage to the animal (Fig. 4*H*).

Discussion

We fabricated EP sensors with Micro-Electro-Mechanical Systems (MEMS) technique to estimate the cortisol hormone changes and record the adrenocortical cellular activities. The EP signal in the adrenal cortex in response to elevated blood ACTH level can be measured. We found that the frequency of the spike was increased within a few seconds to minutes after ACTH administration, especially in the adrenal cortex. Cortisol level and glucose level in the blood were also increased with ascending spike frequencies after ACTH injection. Moreover, when we injected a higher dose of ACTH, the spike frequency greatly increased. These results showed that the probe could be applied to the quantitative stress hormone exocytosis analysis. Such a probe is also applicable to an actual stress model, such as a forced swim test of the freely moving animal. In this case, we found that EP signals in both the medulla and cortex were elevated.

These results show that the probe could be successfully used to record real-time activities of adrenocortical cells. These advantages suggest that such probe cannot only be used to study the adrenocortical system but can also be used to study other hormone organs. In conclusion, this technique may provide a paradigm for the diagnosis and treatment of chronic stress-induced diseases and other adrenocortical hormonal diseases, such as Cushing's disease and Addison's disease. To realize the potential, further research, including a fully implantable wireless power system and an ultra-minimized data transmission system, needs to be performed.

Methods

Details of device fabrication, surgical procedure, device implantation, EP signal measurement, ACTH injection, cortisol and glucose level measurement, cortisol inhibition, forced swim test, freely moving animal test, open field behavior test, and histology test are described in *SI Appendix, Materials and Methods*. All animal studies were performed in accordance with the Korea Food and Drug Administration guidelines. All the animal procedures were approved by the Sungkyunkwan University Institutional Animal Care and Use Committee (permission no. SKKUIACUC-17-1-4-2).

1. Everly G, Lating J (2013) *A Clinical Guide to the Treatment of the Human Stress Response* (Springer, New York).
2. Ehlert U, Gaab J, Heinrichs M (2001) Psychoneuroendocrinological contributions to the etiology of depression, posttraumatic stress disorder, and stress-related bodily disorders: The role of the hypothalamus-pituitary-adrenal axis. *Biol Psychol* 57:141–152.
3. Smith SM, Vale WW (2006) The role of the hypothalamic-pituitary-adrenal axis in neuroendocrine responses to stress. *Dialogues Clin Neurosci* 8:383–395.
4. Gong S, et al. (2015) Dynamics and correlation of serum cortisol and corticosterone under different physiological or stressful conditions in mice. *PLoS One* 10:e0117503.
5. Reagan LP, Grillo CA, Piroli GG (2008) The As and Ds of stress: Metabolic, morphological and behavioral consequences. *Eur J Pharmacol* 585:64–75.
6. Tsigos C, Chrousos GP (2002) Hypothalamic-pituitary-adrenal axis, neuroendocrine factors and stress. *J Psychosom Res* 53:865–871.
7. Wolf OT, Fujiwara E, Luwinski G, Kirschbaum C, Markowitsch HJ (2005) No morning cortisol response in patients with severe global amnesia. *Psychoneuroendocrinology* 30:101–105.
8. Carroll, Curtis GC, Mendels J (1976) Neuroendocrine regulation in depression. I. Limbic system-adrenocortical dysfunction. *Arch Gen Psychiatry* 33:1039–1044.
9. Suvrathan A, Tomar A, Chattarji S (2010) Effects of chronic and acute stress on rat behaviour in the forced-swim test. *Stress* 13:533–540.
10. Zareian P, Karimi MV, Dorneyani G (2011) The comparison of the effects of acute swimming stress on plasma corticosterone and leptin concentration in male and female rats. *Acta Med Iran* 49:284–287.
11. Shi S, et al. (2014) Depression increases sympathetic activity and exacerbates myocardial remodeling after myocardial infarction: Evidence from an animal experiment. *PLoS One* 9:e101734.
12. Stojanovich L, Marisavljevich D (2008) Stress as a trigger of autoimmune disease. *Autoimmun Rev* 7:209–213.
13. Chen Y, Lyga J (2014) Brain-skin connection: Stress, inflammation and skin aging. *Inflamm Allergy Drug Targets* 13:117–190.
14. Marcovecchio ML, Chiarelli F (2012) The effects of acute and chronic stress on diabetes control. *Sci Signal* 5:pt10.
15. Scott KA, Melhorn SJ, Sakai RR (2012) Effect of chronic social stress on obesity. *Curr Obes Rep* 1:16–25.
16. Dallman MF, et al. (2003) Chronic stress and obesity: A new view of "comfort food". *Proc Natl Acad Sci USA* 100:11696–11701.
17. Hamilton LD, Meston CM (2013) Chronic stress and sexual function in women. *J Sex Med* 10:2443–2454.
18. Galanakis M, et al. (2015) The association between stress and sexual dysfunctionality in men and women: A systematic review. *Psychology* 6:1888–1892.
19. Hannibal KE, Bishop MD (2014) Chronic stress, cortisol dysfunction, and pain: A psychoneuroendocrine rationale for stress management in pain rehabilitation. *Phys Ther* 94:1816–1825.
20. Kim K, et al. (2017) Highly sensitive and selective electrochemical cortisol sensor using bifunctional protein interlayer-modified graphene electrodes. *Sens Actuators B* 242:1121–1128.
21. Lee MA, Bakh N, Bisker G, Brown EN, Strano MS (2016) A pharmacokinetic model of a tissue implantable cortisol sensor. *Adv Healthc Mater* 5:3004–3015.
22. Singh A, Kaushik A, Kumar R, Nair M, Bhansali S (2014) Electrochemical sensing of cortisol: A recent update. *Appl Biochem Biotechnol* 174:1115–1126.
23. Kaushik A, Vasudev A, Arya SK, Pasha SK, Bhansali S (2014) Recent advances in cortisol sensing technologies for point-of-care application. *Biosens Bioelectron* 53:499–512.
24. Haemisch A, Guerra G, Furkert J (1999) Adaptation of corticosterone-but not β-endorphin-secretion to repeated blood sampling in rats. *Lab Anim* 33:185–191.
25. Reinhardt V, Cowley D, Scheffler J, Vertein R, Wegner F (1990) Cortisol response of female rhesus monkeys to venipuncture in homecage versus venipuncture in restraint apparatus. *J Med Primatol* 19:601–606.
26. Flow BL, Jaques JT (1997) Effect of room arrangement and blood sample collection sequence on serum thyroid hormone and cortisol concentrations in cynomolgus macaques (*Macaca fascicularis*). *Contemp Top Lab Anim Sci* 36:65–68.
27. Bandulik S, Tauber P, Lalli E, Barhanin J, Warth R (2015) Two-pore domain potassium channels in the adrenal cortex. *Pflugers Arch* 467:1027–1042.
28. Enyeart JJ, Enyeart JA (2013) Ca2+ and K+ channels of normal human adrenal zona fasciculata cells: Properties and modulation by ACTH and AngII. *J Gen Physiol* 142:137–155.
29. Simpson ER, Waterman MR (1988) Regulation of the synthesis of steroidogenic enzymes in adrenal cortical cells by ACTH. *Annu Rev Physiol* 50:427–440.
30. Matthews EK, Saffran M (1973) Ionic dependence of adrenal steroidogenesis and ACTH-induced changes in the membrane potential of adrenocortical cells. *J Physiol* 234:43–64.
31. Kim TI, et al. (2013) Injectable, cellular-scale optoelectronics with applications for wireless optogenetics. *Science* 340:211–216.
32. McCall JG, et al. (2013) Fabrication and application of flexible, multimodal light-emitting devices for wireless optogenetics. *Nat Protoc* 8:2413–2428.
33. Minev IR, et al. (2015) Biomaterials. Electronic dura mater for long-term multimodal neural interfaces. *Science* 347:159–163.
34. Park J, et al. (2016) Electromechanical cardioplasty using a wrapped elasto-conductive epicardial mesh. *Sci Transl Med* 8:344ra86.
35. Donnellan WL (1961) Surgical anatomy of adrenal glands. *Ann Surg* 154:298–305.
36. Kigata T, Shibata H (2017) Anatomical variations of the arterial supply to the adrenal gland in the rat. *J Vet Med Sci* 79:238–243.
37. Chang W, Fang T, Lin Y (2008) Physical characteristics of polyimide films for flexible sensors. *Appl Phys A Mater Sci Process* 92:693–701.
38. Rousche PJ, et al. (2001) Flexible polyimide-based intracortical electrode arrays with bioactive capability. *IEEE Trans Biomed Eng* 48:361–371.
39. Richardson RR, Jr, Miller JA, Reichert WM (1993) Polyimides as biomaterials: Preliminary biocompatibility testing. *Biomaterials* 14:627–635.
40. Lago N, Yoshida K, Koch KP, Navarro X (2007) Assessment of biocompatibility of chronically implanted polyimide and platinum intrafascicular electrodes. *IEEE Trans Biomed Eng* 54:281–290.
41. Seo J, et al. (2004) Biocompatibility of polyimide microelectrode array for retinal stimulation. *Mater Sci Eng C* 24:185–189.
42. Hammond P, Cumming D (2004) Encapsulation of a liquid-sensing microchip using SU-8 photoresist. *Microelectron Eng* 73:893–897.
43. Cho S, et al. (2008) Biocompatible SU-8-based microprobes for recording neural spike signals from regenerated peripheral nerve fibers. *IEEE Sens J* 8:1830–1836.
44. Nemani KV, Moodie KL, Brennick JB, Su A, Gimi B (2013) In vitro and in vivo evaluation of SU-8 biocompatibility. *Mater Sci Eng C* 33:4453–4459.
45. Janjua MZ, Khan MY (1992) Age related changes in the rat adrenal cortex. *J Pak Med Assoc* 42:89–94.
46. Stachenko J, Giroud CJ (1959) Functional zonation of the adrenal cortex: Pathways of corticosteroid biogenesis. *Endocrinology* 64:730–742.
47. Sawada H, Konomi H (1991) The α 1 chain of type VIII collagen is associated with many but not all microfibrils of elastic fiber system. *Cell Struct Funct* 16:455–466.
48. Bressler RS (1973) Myoid cells in the capsule of the adrenal gland and in monolayers derived from cultured adrenal capsules. *Anat Rec* 177:525–531.
49. Magalhães MC, Resende C, Magalhães MM (1978) Effects of cycloheximide on the ultrastructure of the zona fasciculata of the young rat adrenal. *Acta Endocrinol (Copenh)* 88:149–156.
50. Loli P, Berselli ME, Tagliaferri M (1986) Use of ketoconazole in the treatment of Cushing's syndrome. *J Clin Endocrinol Metab* 63:1365–1371.
51. Engelhardt D, Mann K, Hörmann R, Braun S, Karl HJ (1983) Ketoconazole inhibits cortisol secretion of an adrenal adenoma in vivo and in vitro. *Klin Wochenschr* 61:373–375.
52. Tabarin A, et al. (1991) Use of ketoconazole in the treatment of Cushing's disease and ectopic ACTH syndrome. *Clin Endocrinol (Oxf)* 34:63–69.
53. Hamelink C, et al. (2002) Pituitary adenylate cyclase-activating polypeptide is a sympathoadrenal neurotransmitter involved in catecholamine regulation and glucohomeostasis. *Proc Natl Acad Sci USA* 99:461–466.
54. Kotani N, et al. (2001) Preoperative intradermal acupuncture reduces postoperative pain, nausea and vomiting, analgesic requirement, and sympathoadrenal responses. *Anesthesiology* 95:349–356.
55. Gesto M, López-Patiño MA, Hernández J, Soengas JL, Míguez JM (2013) The response of brain serotonergic and dopaminergic systems to an acute stressor in rainbow trout: A time course study. *J Exp Biol* 216:4435–4442.
56. Buske-Kirschbaum A, Geiben A, Höllig H, Morschhäuser E, Hellhammer D (2002) Altered responsiveness of the hypothalamus-pituitary-adrenal axis and the sympathetic adrenomedullary system to stress in patients with atopic dermatitis. *J Clin Endocrinol Metab* 87:4245–4251.
57. Heinrichs M, et al. (2001) Effects of suckling on hypothalamic-pituitary-adrenal axis responses to psychosocial stress in postpartum lactating women. *J Clin Endocrinol Metab* 86:4798–4804.

ENGINEERING

APPLIED BIOLOGICAL SCIENCES